Development of Non-intrusive Fluid Thermometry in Air with Temperature-sensitive Particles by Two-gated Method

Kosuke Fujiwara[1, 2*], Konstatinos Kontis[1], Takeomi Ideta[2]

[1]School of Engineering, University of Glasgow, Glasgow, United Kingdom
[2]Technology Platform Centre, IHI Corporation, Yokohama, Japan
*corresponding author: k.fujiwara.1@research.gla.ac.uk

Abstract A non-intrusive fluid thermometry technique using in-house temperature-sensitive particles by means of two-gated method was demonstrated. In the present research, phosphorescence signals were integrated over exposure time that was much longer than the phosphorescence, thus lower frame rate could be used to avoid faster frame rate which would have compromised spatial resolution. Ruthenium-based temperature-sensitive particles were scattered in a heated turbulent jet emanating from a pipe and its phosphorescence was captured by a sCMOS camera in double-frame mode. Calibration function for temperature vs. intensity ratio between 1st and 2nd frame of the double-frame images was generated by two means: static calibration using a sample on a temperature-controlled surface and dynamic calibration using the potential core of the heated jet. Calibration function of the dynamic case was used to convert the raw images to instantaneous thermal captions, and the thermal captions exhibited typical flow characteristics of a heated turbulent pipe jet such as hot potential core, and low-temperature shear layer with fine-scale structures. The average temperature field of the present demonstration agreed well with temperature distribution measured by conventional T-type thermocouple, confirming the accuracy of the technique. Using 95%-confidence level, the uncertainty in temperature was evaluated to be ±4.9°C at the jet temperature of 96.3°C. Future work is to investigate the factors that contribute to the uncertainty to improve accuracy and precision of the technique.

Keywords: Temperature-sensitive Phosphors, Fluid Thermometry, Non-intrusive Measurement

1. Introduction

Thermal energy within fluid is transferred by convection and conduction. In most cases, the flow of interest is turbulent and therefore transfer of energy by the convection is prevalent. A measure of convective heat transfer between fluid and a surface exposed to the fluid is usually represented by the coefficient of convective heat transfer or its non-dimensional form, Nusselt number which are highly dependent on flow dynamics. One example is gas turbine blades; it applies film-cooling to reduce thermal load on a surface as well as internal cooling to remove as much heat from the blade as possible. For film cooling, according to Goldstein [1], the distribution of surface temperature and coefficient of heat transfer is affected by fluid-dynamical and geometric factors. Fluid-dynamical factors include freestream velocity (represented by Reynolds number), injection rate (represented by blowing ratio or momentum ratio), and geometric factors include geometry and arrangement of injection holes for example. In the process of thermal design, an empirical coefficient of convective heat transfer is used, however, the coefficient can only predict temperature or heat flux, but provides few information on the flow itself.

Advances in computations have enabled and inspired researchers to investigate the details of convective heat transfer. Computational Fluid Dynamics (CFD) has become an indispensable tool which can provide full three-dimensional information on the flow field such as flow velocity, pressure, temperature, and concentration. Recent CFD regarding film cooling nowadays covers transient cases using Large-Eddy Simulation (LES) [2]-[4] where the unsteadiness and fine-scale vortices are captured. Whilst CFD enhances the understanding in the flow dynamics, it also requires deep knowledge and skills to conduct a proper simulation. This includes the selection of a turbulence model, numerical scheme, discretization, boundary condition, and post-processing of massive data [5]-[8]. Of these, boundary condition can significantly affect the quality of numerical results, especially for LES, thus requires careful setting and reasoning. However, measurement of boundary conditions is not easy and information is always limited. Moreover, CFD must always be compared and validated with experimental data to ensure its quality.

In this context, it is crucial to develop experimental techniques which can provide as much information as possible. Measure of thermal energy is temperature and perhaps thermocouple comes as a very first

option. It is a well-established method that is easy, quick, and precise, however, its measurement is limited only at a single point and the probe has to be traversed to obtain spatial distribution of temperature. Moreover, this technique is destined to interfere with the flow, which can alter the nature of the flow, destroying the whole purpose of the measurement itself. To avoid the undesired interference, non-intrusive thermometry technique apparently is preferred. Infra-red (IR) camera is a well-known non-intrusive thermometer based on radiative heat transfer. Present IR camera and system are commercially available [9] and basically ready to be used once purchased. However, it can only capture temperature of a surface and provides no direct information on the flow. Its results are also prone to emissivity of an object, reflection, and ambient condition, therefore careful calibration is necessary to conduct a precise measurement. Laser-Induced Fluorescence (LIF) is a non-intrusive thermometry technique which is based on temperature-dependent fluorescence intensity of a chemical compound seeded in a flow. A combination of Rhodamine-B/Rhodamine-110 were used in water by Sakakibara at al. [10][11] and acetone in air flow by Shi et al. [12]. However, this technique is limited by the nature of fluorescent compound. For example, Rhodamine-B/Rhodamine-110 can only be dissolved in a liquid of polar molecules like water, thus cannot be used in non-polar solvent such as oil. Acetone is combustible, therefore cannot be used under combusting environment although LIF certainly is an excellent technique to non-intrusively measure fluid temperature.

More recently, non-intrusive thermometry applies temperature-sensitive phosphors. The fundamental principle of the phosphors, like LIF, is based on their luminescence (phosphorescence) intensity that is temperature-dependent. There is a wide spectrum of existing phosphors [13]-[16] depending on temperature range and they are usually provided in a small quantity of particulates. Temperature-sensitive paints (TSP) are formed when one of the phosphors selected is mixed with a solvent and a binder at a certain formulation and dried well upon painting. Kontis [17] measured surface temperature inside a model rectangular supersonic combustor using Dy3+:YAG phosphor and demonstrated its applicability at high-speed environment. Nau et al. [18] used YAG:Dy and YAG:Eu to measure wall temperature in a gas turbine model combustor with sooting flames at an elevated pressure and temperature. For real machinery, Someya et al. [19] measured wall temperature inside an engine cylinder and Seyfield et al. [20] measured temperature on the outlet nozzle of Volvo RM12 fighter jet engine.

In order to conduct measurement of fluid temperature rather than that of surface temperature, recent investigations apply fine power of phosphor, or temperature-sensitive particles. However, because the particles are moving with surrounding fluid, intensity-based method used in TSP cannot be used, therefore either two emission lines or temporal information is used to convert signal intensity to temperature information. Abram et al. [21] conducted thermometry in a heated turbulent jet up to around 400K by taking the intensity ratio of two different emission wavelength of BAM:Eu particles. Similar techniques involving two emission lines are conducted with Pr:YAG up to 750K by Jordan et al. [22]. Whilst the proposed techniques cover from room temperature to high temperature in gaseous fluid, the techniques require at least two cameras (not cheap) equipped with proper optical filters to separate two different emission lines and the cameras basically need to capture the identical field of view at a pixel-by-pixel level. Lifetime-based technique rather than two-emission line is also proposed in literature. The lifetime-based method utilizes the temporally-decaying phosphorescence which is specific to the phosphor. Someya et al. [23] prepared an in-house Eu:TTA-based temperature-sensitive particles and only with a single high-speed camera, they successfully conducted fluid thermometry in silicone oil. Although the advantage of the technique is that it only requests one single camera, the limitation comes when the time scale of fluid motion becomes comparable with that of the decay of phosphorescence. In such case, captured images would have "elongated" particles that are in motion during camera exposure. In general, gas flow has much larger flow velocity than liquid flow, therefore a phosphor with shorter decay time is certainly preferred to prevent the elongation phenomenon. However, a shorter decay time means that the lifetime method requires a camera with faster frame rate which compromises pixel resolution and signal intensity.

To overcome the issues with the lifetime-based method, this paper demonstrates a fluid thermometry technique in a low-speed air jet with temperature-sensitive particles by means of two-gated method, rather than the "direct" lifetime method. The demonstration was conducted by using in-house Ruthenium-based temperature-sensitive particles seeded in a heated jet emanating from a pipe. Measurements were made in the jet from room temperature up to 100°C. By two-gated method unlike the lifetime method, phosphorescence signals were integrated over longer exposure time, thus a luminophore with shorter decay time can be used without selecting faster frame rate. A double-frame camera with very short inter-frame time was implemented to capture two consecutive images whose ratios were then taken to be converted to temperature

map in the post-process. Calibration was conducted by using the luminophore on a temperature-controlled surface (static calibration) and the potential core of the jet (dynamic calibration) and the result is discussed.

2. Temperature-sensitive Particle

In order to measure the temperature of a fluid, temperature-sensitive luminophore has to exist in the fluid to behave as a sensor, and henceforward temperature-sensitive particles were prepared in the present experiment. The phosphor was a ruthenium complex, namely tris (2, 2'-bipyridine) ruthenium (II) chloride, [Ru(bpy)3]Cl2 (Sigma Aldrich) whose decay time is in the order of 1-10μs at room temperature [24]. Porous fine particles of SiO_2 (B6-C Godd Ball, Suzuki Yushi, JAPAN) were soaked in a weak solution of the phosphor, and the sediment was dried very well until it again became a powder. To quantify the ability of the particle to follow the fluid motion, Stokes number defined by (1) was calculated.

$$St = \frac{\rho_p d_p^2 u}{18\mu L} \tag{1}$$

In the equation, ρ_p, d_p, u, μ, and L represent the density of the particle, the diameter of the particle, flow velocity, viscosity of the fluid, and representative length scale respectively. Pipe diameter (d=15.8mm) was taken as the representative length scale and based on the present experimental condition, Stokes number was calculated to be St=0.017 << 1, therefore the generated particle follows the motion of fluid very well.

Thermometry using temperature-sensitive particles are tacitly based on thermal equilibrium between the particle and the fluid surrounding the particle, i.e., the particle suspended in the fluid instantaneously reflects the temperature of the fluid. Therefore, the time scale of heat transfer from fluid to particle and that of heat transfer of turbulent motion were also quantified. To calculate the time scale of the former, lumped heat model using the coefficient of convective heat transfer with Ranz-Marshal's [25] correlation was used. In the present paper, the time it takes for the particle to reach 99% of ambient fluid was used and based on experimental condition, the time scale is calculated to be 1.3μs. This value is much shorter than the time scale of heat transfer by turbulent motion which is d/u=1.62ms. This means that the heat is transferred by conduction almost instantaneously before the heat is transported by the convection, therefore, the prepared particle is suitable for seeding and measuring temperature distribution of the flow.

Non-intrusive thermometry technique utilizes physical chemistry of a phosphor. A phosphor is excited with an external light source that corresponds to its certain energy transition. Then, it emits wavelength which is longer (thus lower energy) than the original light source when returning to its ground state via some energy levels, depending on phosphor. This process takes certain amount of time, which is temperature-dependent. Temporal behavior of this process is modeled by an exponential function,

$$I(x, y, t) = I_o(x, y) \exp\left[-\frac{t}{\tau(T)}\right] \tag{2}$$

where the intensity of phosphorescence at t=0 and temperature-dependent decay constant are represented by I_o and $\tau(T)$ respectively. $I_o(x,y)$ is a function of position (or pixel on camera) because there is local variation in energy input, spatial density of the phosphor particulate, and optical orientations, all of which are virtually impossible to control. Therefore, I_o must be eliminated from the equation by taking ratio against a reference image. However, since the phosphor is in particulate form in the present paper, it is impossible to have the particles at the identical positions in every single snapshot, therefore intensity-based method is not possible.

In order to such difficulty, the present technique applied two-gated method. Two consecutive images separated by very short interval were captured and this mathematically corresponds to the integration of (2). Mathematical representations of the integration of 1st and 2nd image are calculated in (3) and (4) respectively. The schematic of timing diagram of the method is illustrated in Fig.1.

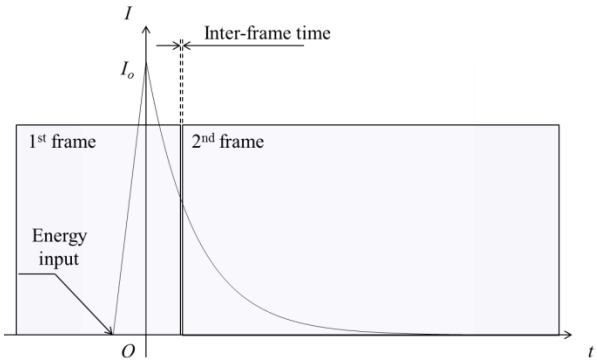

Fig.1. Timing diagram

$$\int_{t_1}^{t_2} I_1(t)dt = \int_{t_1}^{t_2} I_o \exp\left[-\frac{t}{\tau(T)}\right] dt = I_o\left(\exp\left[-\frac{t_1}{\tau(T)}\right] - \exp\left[-\frac{t_2}{\tau(T)}\right]\right) \quad (3)$$

$$\int_{t_3}^{t_4} I_2(t)dt = \int_{t_3}^{t_4} I_o \exp\left[-\frac{t}{\tau(T)}\right] dt = I_o\left(\exp\left[-\frac{t_3}{\tau(T)}\right] - \exp\left[-\frac{t_4}{\tau(T)}\right]\right) \quad (4)$$

Taking the ratio of the 2nd frame to the 1st frame yields the temperature-dependent function represented by (5) where the only variable is the $\tau(T)$ and the calibration function $f(T)$ was experimentally generated.

$$\frac{\int_{t_3}^{t_4} I_2(t)dt}{\int_{t_1}^{t_2} I_1(t)dt} = \frac{\exp\left[-\frac{t_3}{\tau(T)}\right] - \exp\left[-\frac{t_4}{\tau(T)}\right]}{\exp\left[-\frac{t_1}{\tau(T)}\right] - \exp\left[-\frac{t_2}{\tau(T)}\right]} = f(T) \quad (5)$$

3. Experimental Method and Condition

In the present paper, static and dynamic calibrations were conducted, and the measurement system is illustrated in Fig.2. It consists of scientific CMOS camera (Imager sCMOS, Lavision), a long-pass high-performance optical filter (#84-757, Edmund Optics), second harmonics of Nd:YAG double-cavity laser (λ_{ex}=532nm, NS65-15, Litron), synchronizer, and commercially-available software Davis 10 (Lavision). For static calibration, a 1cm×1cm aluminum sample was coated with phosphor and placed on a Peltier device which was controlled from 16.8°C up to 97.8°C. Single shots of laser were directed on the sample and the phosphorescence was captured by the sCMOS, where optimum timing to capture double-frame images was found by trial and error. For dynamic calibration and thermometry of turbulent jet, its apparatus is illustrated in Fig.3. The flow was driven by pressurized air from the compressor and its volume flow rate was measured by the flow meter after which the flow was seeded with the in-house particles. Before the pipe exit, the flow was heated by the inline heater (AHP-7562, Omega Engineering) from T_j=17.1~96.3°C for both calibration and measurement of the turbulent heated jet. The jet temperature was recorded by a ϕ0.5mm T-type thermocouple located at the center of the jet exit. The measurement system was identical to the one used in the static calibration with one exception, i.e. a laser sheet optics (f=-20mm) making 2mm-thick laser sheet towards the pipe jet. The pipe had a diameter of d=15.8mm and the volume flow rate was fixed at 85 Normal-L/min. which gave an exit jet velocity of u=9.8m/s. The summary is shown in Table.1.

The laser pulses were shot at 10Hz and a full power of 210mW with fluctuation of 1.1%. The camera operated at the same frequency to the laser and a full resolution of 2560×2160pix^2. The size of physical domain was approximately 74.2mm wide in the pipe-radial direction and 87.9mm long in the streamwise direction. The exposure time of the 1st and 2nd image had fixed values of 15μs and 19.8ms respectively and a fixed inter-frame time of 120ns. An in-house MATLAB code was developed and average of background image was then taken and subtracted from raw 1st and 2nd images. After the subtraction, pixels lower than 20-count was recognized as a pixel without particle and thus was evaluated as ambient temperature. Digital binning with the window size of 8×8pix^2 to increase virtual signal intensity was implemented and the final

spatial resolution of the thermal field was 275μm/pix.

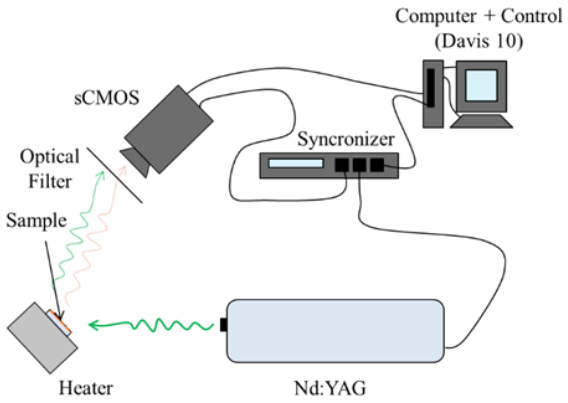

Fig.2. Static calibration

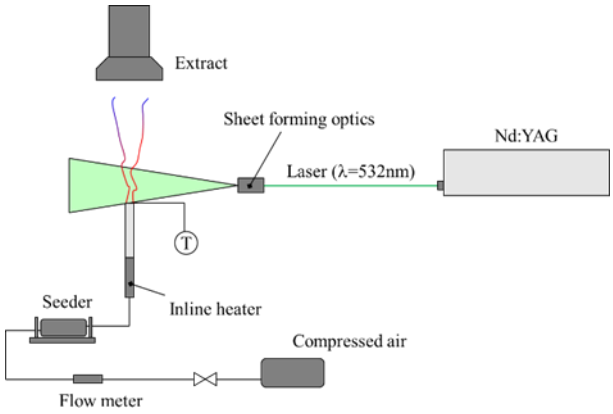

Fig.3. Dynamic calibration and measurement

Table.1. Summary of experimental conditions

-	Temperature	Jet exit velocity
	T_j [°C]	u_j [m/s]
Static	16.8~97.8	-
Dynamic	17.1~96.3	9.8

4. Results and Discussion

At first, the results of static and dynamic calibration are shown in Fig.4. The calibration functions fitting to the data points were formed by $f = ax^b$(a and b are constants) and are shown by the dotted or solid line for static and dynamic cases respectively.

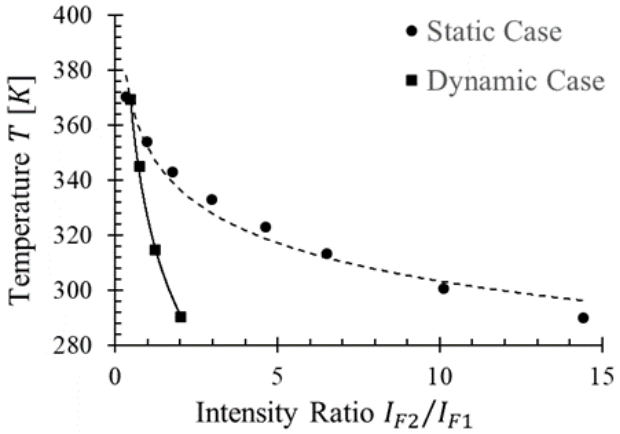

Fig.4. Dynamic calibration and measurement

Using the principle of propagation of uncertainty [26][27], the uncertainty in temperature was calculated to be ±1.4°C at T_j=16.8°C and ±6.3°C at T_j=97.8°C for static case, and ±1.9°C at T_j=17.1°C and ±4.9°C at T_j=96.3°C for dynamic case using 95%-confidence level. As is in the graph, in both cases, the ratios between signal intensity of 1st and 2nd images vary with temperature, and therefore the present particle is certainly temperature-sensitive. However, the results of static and dynamic cases differ by large extent. The static case has larger ratio than the dynamic case; the former has almost 7 times as large at the lowest temperature. It is suspected that the disagreement was caused by differences in optical conditions such as distance and angle between the measurement zone and the camera chip which can potentially affect absolute signal intensity through which the ratio was affected. From the empirical correlations, it is readily anticipated that such

difference would yield unphysical result when the calibration function of static case *were* implemented to the snapshots of dynamic cases (or vice versa). For example, around 290K, the ratio for dynamic case is around I_{F2}/I_{F1}=2 whereas the static case is around I_{F2}/I_{F1}=14.5. The dynamic case does not have value at I_{F2}/I_{F1}=14.5 or the extrapolated value would yield much lower temperature of 211K. This is thermodynamically impossible and it is for this reason the static one will be discarded in the further discussion.

Fig.5 illustrates a typical instantaneous distribution of temperature with the jet at T_j=96.3°C. Both radial and streamwise directions are normalized by pipe diameter d, and temperature is normalized by jet and ambient temperatures by (6).

$$\eta = \frac{T - T_{amb}}{T_j - T_{amb}} \tag{6}$$

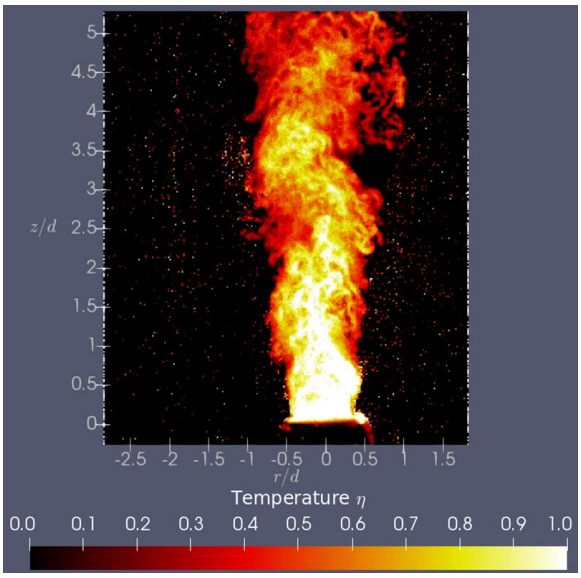

Fig.5. Instantaneous snapshot

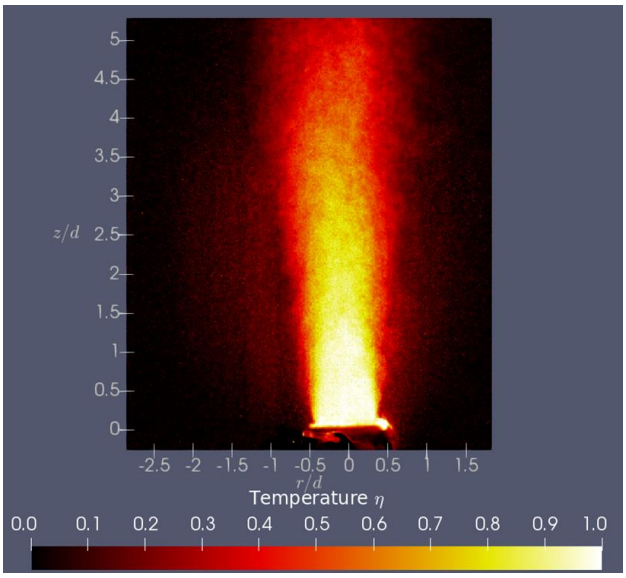

Fig.6. Average distribution

As it is demonstrated in Fig.5, the hot jet exits the pipe at high temperature and maintains the hot core downstream until around z/d=1.5. In the region of 2.5<z/d<3.5 and -0.5<r/d<0, the hot core is being torn apart by the turbulent motion and transported downstream, too. A shear between the jet and static ambient air generated instability and the growth of turbulent shear with fine-scale structures is well visualized by the decrease in the temperature in the shear. Since only the jet was seeded with the temperature-sensitive particles, the measurement was physically impossible for the region well outside the jet, which is illustrated by the dark regions outside the jet.

Fig.6 illustrates distribution of average temperature of the snapshots. In the averaged thermal image, shrinkage of potential core in the streamwise direction as well as growth of shear between the jet and ambient air are clearly visualized. In order to quantitatively demonstrate the accuracy of present data, a T-type thermocouple was inserted in the flow to obtain temperature. The thermocouple was traversed by a spatial increment of 0.5d along the centerline of the pipe (z/d=0) and the comparison is shown in Fig.7. As it is in the graphs, the present non-intrusive technique agrees well with the thermocouple. In the figure, temperature maintains value above η=0.9 until around z/d=1.5 and the rate of decrease in temperature increases a after this point, suggesting the termination of the potential core of the heated jet around this location. The agreement with the thermocouple in general continues all the way down to the streamwise edge of the averaged thermal image. The thermal distribution obtained by present non-intrusive thermometry contains spatial high-frequency noise, which may be removed by adding another filter in the future.

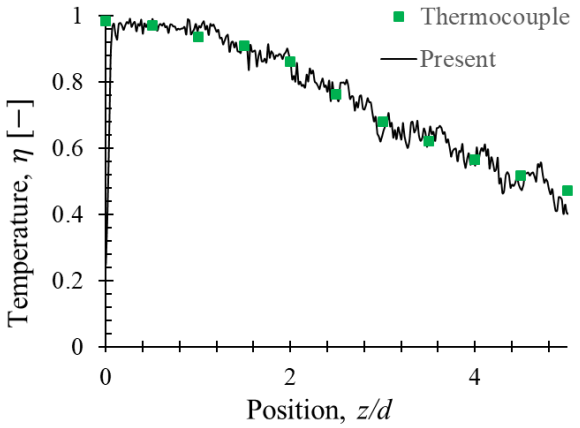

Fig.7. Comparison with a thermocouple

5. Conclusion and Future Work

A fluid thermometry technique with temperature-sensitive particles by means of two-gated method, rather than the "direct" lifetime method, has been attempted. In the present thermometry technique, phosphorescence signals are integrated over exposure time that is much longer than the phosphorescence itself. This method enables to choose a phosphor with shorter decay time, so that a faster frame rate which compromises spatial resolution of the camera does not have to be selected. In-house Ruthenium-based temperature-sensitive particles developed in-house and a heated jet emanating from a pipe was measured by the particle. The particles were excited by a high-power Nd:YAG laser, the phosphorescence was captured by a sCMOS camera in double-frame mode. Calibration function of temperature vs. intensity ratio between 1st and 2nd frame of the double-frame images was generated by two means: static calibration with a sample on a temperature-controlled surface and dynamic calibration using the potential core of the heated jet. Measurements were conducted in a turbulent pipe jet at 9.8m/s (Re_d=7.1×10^3) which was heated from 17.1°C up to 96.3°C. Two-gated method captured two consecutive images which was successfully converted into temperature field by taking their ratio. However, calibration functions by static calibration and dynamic calibration did not agree at all and the difference was found to be as large as 7 times with the static case being the larger one. Therefore, the calibration function from the static case was discarded. It is suspected that such difference was caused by difference in optical conditions

The present instantaneous captions exhibited the typical flow characteristics of a heated turbulent pipe jet such as hot potential core, low temperature shear, and regions that was being torn apart from the core due to turbulent motions. The present results had final spatial resolution of 275μm/pix and fine-scale structures in the turbulent shear were captured well, too. The average temperature field of the present demonstration agreed well with temperature distribution measured by conventional T-type thermocouple, proving the validity of the present thermometry technique. The uncertainty in temperature which was estimated to be ±1.9°C at T_j=17.1°C and ±4.9°C at T_j=96.3°C using 95%-confidence level. The present results also contained high-frequency spatial noise. These may be eliminated by strengthening signal intensity and using a more enhanced de-noising algorithm; however, further research is necessary to investigate the factors that contribute to uncertainty in the measurement technique.

References

[1] Goldstein R J (1971) Film Cooling, In: Advances in Heat Transfer vol. 7, pp.321-379
[2] Schneider H, Terzi D, Bauer H J (2012) Turbulent Heat Transfer and Large Coherent Structures in Trailing-edge Cutback Film Cooling. *Flow Turbulence and Combustion*, vol. 88, pp.101-120
[3] Tyagi M, Acharya S (2003) Large Eddy Simulation of Film Cooling Flow From an Inclined Cylindrical Jet. *Journal of Turbomachinery* vol. 125
[4] Sarkar S, Babu H (2015) Large Eddy Simulation on the Interactions of Wake and Film-Cooling Near a Leading Edge. *Journal of Turbomachinery* vol. 137

[5] Tyacke J C and Tucker P G (2015) Future Use of Large Eddy Simulation in Aero-engine. *Journal of Turbomachinery* vol. 137
[6] Tucker P G (2013) Trends in turbomachinery turbulence treatments. *Progress in Aerospace Sciences* vol. 63, pp.1-32
[7] Tucker P G (2011) Computation of unsteady turbomachinery flows: Part 1 – Progress and challenges. *Progress in Aerospace Sciences* vol. 47, pp.522-545
[8] Tucker P G (2011) Computation of unsteady turbomachinery flows: Part 2 – LES and hybrids. Progress in Aerospace Sciences, pp.546-569
[9] FLIR, https://www.flir.com/
[10] Sakakibara J, Adrian R J (1999) Whole field measurement of temperature in water using two-color induced fluorescence. *Experiments in Fluids* vol. 26 pp.7-15
[11] Sakakibara J, and Adrian R J (2004) Measurement of temperature field of a Rayleigh-Benard convection using two-color laser-induced fluorescence. *Experiments in Fluids* vol. 37, pp.331-340
[12] Shi L, Yu Z, Jaworski A J (2010) Application of laser-based instrumentation for measurement of time-resolved temperature and velocity fields in the thermoacoustic system. *International Journal of Thermal Sciences* vol. 49, pp.1688-1701
[13] Khalid A H, Kontis K (2008) Thermographic Phosphors for High Temperature Measurements: Principles, Current State of the Art and Recent Applications. *Sensors* vol. 8
[14] Alden M, Omrane A, Richter M, Sarner G, Thermographic phosphors for thermometry: A survey of combustion applications. *Progress in Energy and Combustion Science* vol. 37, pp.422-461
[15] Brubach J, Kissel T, Frotscher M, Euler M, Albert B, Dreizler A (2011) A survey of phosphors novel for thermography. *Journal of Luminescence* vol. 131, pp.559-564
[16] Brubach J, Pflitsch C, Dreizler A, Atakan B A (2013) On surface temperature measurements with thermographic phosphors: A review. *Progress in Energy and Combustion Science* vol. 39, pp.37-60
[17] Kontis K (2003) Surface Heat Transfer Measurements Inside a Supersonic Combustor by Laser-Indued Fluorescence. *Journal of Thermophysics and Heat Transfer* vol. 17 no.3
[18] Nau P, Yin Z, Geigle K P, Meier W (2017) Wall temperature measurements at elevated pressures and high temperature in sooting flames in a gas turbine model combustor. *Applied Physics B*
[19] Someya S, Okura Y, Munakata T, Okamoto K (2013) Instantaneous 2D imaging of temperature in an engine cylinder with flame combustion. *International Journal of Heat Mass Transfer* vol. 62, pp.382-390
[20] Seyfried H, Sarner G, Omrane A, Richter M, Schmidt H, Alden M, (2005) Optical Diagnostics for Characterization of a Full-size Fighter-jet Afterburner. ASME Turbo Expo 2005, GT2005-69058
[21] Abram C, Fond B, Heyes A L, Beyrau F (2013) High-speed planar thermometry and velocimetry using thermographic phosphor particles. *Applied Physics B* vol. 111, pp.155-160
[22] Jordan J, Rothamer D A (2013) Pr:YAG temperature imaging in gas-phase flows. *Applied Physics B* vol. 110, pp.285-291
[23] Someya S, Li Y, Ishii K, Okamoto K (2010) Combined two-dimensional velocity and temperature measurements of natural convection using a high-speed camera and temperature-sensitive particles. *Experiments in Fluids* vol. 50, pp.65-73
[24] Liu T, Sullivan J P (2005) Pressure and Temperature Sensitive Paints, Springer
[25] JSME Textbook (2006) Heat Transfer, pp.88
[26] Kline S J and McClintock F A (1953) Describing UNCERTAINTIES in SINGLE-SAMPLE EXPERIMENTS, In: Mechanical Engineering
[27] Mofat R J (1988) Describing the Uncertainties in Experimental Results. *Experiments in Thermal and Fluid Sciences* vol. 1